JOURNAL OF MATERIALS SCIENCE **38** (2003) 2709–2716

Innovative processing and mechanical properties of high temperature syntactic foams based on a thermoplastic/thermoset matrix

T. FINE*, H. SAUTEREAU
Laboratoire des Matériaux Macromoléculaires UMR CNRS 5627, Institut National des Sciences Appliquées de Lyon-69621 Villeurbanne Cedex, France
E-mail: thomas.fine@insa-lyon.fr

V. SAUVANT-MOYNOT
Institut Français du Pétrole, BP 3-69390 Vernaison, France

An innovative processing of syntactic foams based on high-glass transition temperature thermoplastic is reported. The aim is to propose an insulating material able to withstand both continuous effluent temperature up to 150°C and hydrostatic pressure up to 300 bar. Uniaxial compression and tension tests have been performed. Two factors seems to govern the mechanical properties: the wall thickness/radius ratio (e/r) and the volume fraction of microspheres. At room temperature, the study of the strain recovery at the yield stress shows that the plastic deformation is negligible compared to the elastic and anelastic part. The study of the yielding behavior at room temperature has shown a large influence of the type of microsphere compared to the influence of the volume fraction. The syntactic foams exhibit good performance at 150°C as expected from the matrix selection. Comparison with a few classical models have been done.

1. Introduction

The offshore exploitation and conveying of oil and gas resources in deep water require the use of insulated pipelines in order to prevent the crude oil or natural gas from producing waxes or hydrates. If the pipeline temperature drops too low, heavy components in crude oil can solidify into waxy material that can clog the line, and natural gas can form hydrates that can also cause pipeline blockage. Deep water wells put stringent requirements on insulation products to withstand compressive loads and to offer heat loss resistance. Syntactic foams have been identified as suitable insulating materials for this application. Syntactic foams are composite cellular materials obtained by embedding hollow spherical particles (called microspheres or microballons) in a polymer matrix. Therefore, syntactic foams exhibit an artificially closed porosity made of stiff hollow particles, whereas classical foams foamed by using a blowing agent (chemical or physical gas expansion) may sometimes exhibit interconnected cavities. This peculiarity allows syntactic foams to support higher compressive strength than cellular foams do. This is why syntactic foams, commonly used in buoyancy applications in deep water [1–3] are nowadays considered as suitable insulating materials up to 80°C. However, high temperature fields (>120°C) constitute a new range of application, so there is a need for innovative insulating materials for use at high temperatures. In this study, we tried to develop a new process leading to syntactic foam able to withstand both continuous effluent temperature up to 150°C and hydrostatic pressure up to 300 bar.

The starting point of this work is the choice of a thermostable matrix based on the polyphenylene ether (PPE), one of those "intractable" amorphous thermoplastic polymers with a glass transition temperature around 200°C and whose transformation is made by the use of a reactive solvent [4–6].

Another expected advantage associated with the choice of a thermoplastic matrix is the higher toughness exhibited compared to thermoset brittleness. Indeed, the insulation system must be able to withstand the extreme squeeze loads of the tensiometer that is used for deep water laying of pipeline. On the contrary, careful attention has to be paid to the processing of a syntactic foam since the mixing of microspheres with a thermoplastic material above T_g may partly break microspheres and so reduce the final expected properties. In fact, syntactic foams are mainly prepared by using a thermoset matrix because of the favourable related processing conditions avoiding breakage by gently blending the hollow microspheres with the thermoset precursors of very low viscosity [7]. Nevertheless, some attempts have been made to process syntactic foams with a thermoplastic matrix by using a solvent [7], or even by using a twin-screw extruder [8, 9].

*Author to whom all correspondence should be addressed.

The objective of the present article is to report on

1. The innovative processing of syntactic foams based on high-T_g thermoplastic;
2. The morphological characterisation of those syntactic foams by scanning electron microscopy;
3. The mechanical properties of the syntactic foams prepared (elasticity and deformation at the yield point at room temperature, plasticity at room temperature and at 150°C). The results are discussed in terms of the glass hollow microspheres used and the volume fraction. The glass microspheres are not silane treated in that work which is mainly focus on static properties and not with long term ageing under pressure in salted water.
4. Our attempt to fit the elastic behaviour of the syntactic foams by using two-phase models.

Priority is given in this work to the validation of the technology developed and to the evaluation of the mechanical performance up to 150°C of the related foams. Other properties of the syntactic foams and their optimisation is currently the matter of additional investigations.

2. Experimental

2.1. Materials

The formula, characteristics and origin of the chemicals used in this study are given in Table I for the components of the matrix, namely the thermoplastic PPE and the thermoset precursors DGEBA and MCDEA mixed in stoichiometric proportions. The origin and characteristics of the hollow glass spheres (microspheres) tested are reported in Table II as given by suppliers in technical data sheets. Note that their surfaces were not treated.

2.2. Processing

The syntactic foams were prepared in a two-step process: the first one was the reactive extrusion of PPE in order to prepare the reactive blend to be used as matrix, the second one aimed at dispersing the hollow glass spheres in the matrix.

i) The reactive extrusion of high-T_g thermoplastics has been extensively studied by Venderbosch *et al.* [6] and optimised by Bonnet *et al.* [4, 5]. The principle is the dissolution of the high-T_g thermoplastic (TP) in thermoset (TS) precursors during a one-stage extrusion process [5] in a twin-screw extruder around 180°C. A homogeneous processable blend with intermediate T_g and very low epoxy conversion is collected out of the extruder, quenched in the air and cut into pellets. Under cure, the reactive blend exhibits phase separation at a given conversion induced by molar mass increasing through reaction of the thermoset precursors [10]. A variety of morphologies can be generated within the fully cured material, and they mainly depend on the initial amount of TP, ϕ_{TP}, with respect to the critical

TABLE I Characteristics of the chemicals used

Name	Formula	Suppliers
4,4′-Methylenebis [3-chloro 2,6-diethylaniline]	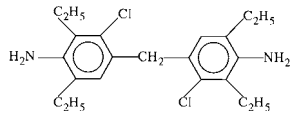	Lonza
MCDEA	$M = 380\ g \cdot mol^{-1}$	
Diglycidyl ether of bisphenol A	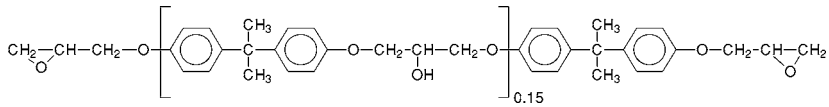	Vantico LY556
DGEBA $\bar{n} = 0.15$	$\overline{M_n} = 382.6\ g \cdot mol^{-1}$	
Polyphenylene ether	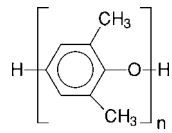	General Electric PPE 820
PPE	$\overline{M_n} = 12000\ g \cdot mol^{-1}$ $\overline{M_w} = 25000\ g \cdot mol^{-1}$ $T_g = 220°C$	

TABLE II Microsphere characteristics (data from the technical sheet given by suppliers)

Microsphere references	Suppliers	Median diameter[a] (50% vol) (μm)	Theoretical wall thickness e (μm)	True density ρ_{true} (kg/m^3)	Variation of apparent density $\rho_{apparent}$ (kg/m^3)	Typical isostatic crush strength	
						Test pressure (bar)	Target fractional survival (90%)
K25	3M	55	0.93	250	130–180	52	96
S38		40	1.05	380	190–280	280	94
S60		30	1.29	600	310–430	690	92
110P8CP00	Potters	8	0.69	1000	—	1550	83

[a]Particle size distribution was checked using laser diffraction equipment (Malvern Mastersizer 2000).

composition, $\phi_{TP,crit}$ (about 20% by wt of PPE) [11]. If ϕ_{TP} is less than $\phi_{TP,crit}$, the final morphology consists of a dispersion of TP-rich particles in a TS-rich matrix. In the opposite case, when ϕ_{TP} is greater than $\phi_{TP,crit}$, a dispersion of the TS-rich nodules in a TP-rich matrix is obtained. Since we were interested in the properties of a TP matrix, in particular thermal resistance and high toughness, we worked with ϕ_{TP} greater than $\phi_{TP,crit}$.

ii) In the second step, microspheres are incorporated into the reactive blend. An efficient mixing with a minimum amount of resulting crushed microspheres requires processing conditions where the reactive blend exhibits a minimum viscosity. As was shown in the literature [5], the viscosity of the reactive blend increases drastically when the phase separation occurs. For this reason, we chose a matrix composition whose phase separation time gives enough time to produce the mixture TP/thermoset precursors/microspheres at the temperature of extrusion (175°C). According to the results of Poncet *et al.* [12], we decided to use a blend containing 40% wt of PPE (design at PPE40). PPE40 neat material was cured for 2 h at 200°C and post-cured for 2 h at 220°C.

The TP/TS precursors/microspheres blends were made in a Rheomix 600 Haake mixer ($V = 80 \times 10^{-6}$ m^3) for practical use, in comparison to a twin-screw extruder. The set temperature was 175°C, the measured one was around 187°C and the rotation speed of the blades was 80 rpm. The matrix pellets prepared as described in the first step were mixed for 7 min before incorporating the microspheres, and then mixed further for 10 min. We checked that the separation phase had not occurred before the end of the 17 min by following the torque. The composite foams were cured for 2 h at 200°C and 2 h at 220°C.

3. Measurements

Morphologies were characterised on a JEOL 840 Scanning Electronic Microscope (SEM) after gold sputtering on cryofractured surfaces.

The content of broken microspheres in weight percent was determined after calcination (3 h at 500°C under O_2) and immersion in a solvent allowing the separation between broken and unbroken microspheres by decantation (water was used classically, except for Potters microspheres where chloroform was used).

Glass transition temperatures were determined by Differential Scanning Calorimetry (Mettler DCS30 TC10A/TC15) at the onset of the curve drop (heating rate = 10 K · min^{-1}).

The uniaxial compression behavior of parallelepipedic specimens (section 5 × 8 mm^2, height 15 mm) was investigated on a MTS 2/M testing machine to determine the yield stress (σ_y) and the Young's modulus (E). The evolution of the recovered strain after unloading was recorded to highlight the different parts of the deformation (elastic, anelastic, and plastic). Samples were compressed up to a total deformation $\varepsilon_{total} = \varepsilon_y$ (strain at the yield stress σ_y) at a crosshead speed of 1 mm · min^{-1} ($\dot{\varepsilon} = 1.10^{-3}$ s^{-1}). The load was then quickly suppressed (50 mm · min^{-1}) and the deformation was recorded as a function of time. The remaining deformation after 60 min was considered as the plastic deformation ε_{pl}. The elastic value ε_{el} was calculated from the ratio of $\sigma(\varepsilon_{total})$ to Young's modulus.

Young's modulus and Poisson's ratio ν were measured in uniaxial tensile test at 25°C on an Instron 4469 testing machine with parallelepipedic specimens (section 15 × 5 mm^2) with bonded Micro-Measurements precision strain gages, giving both longitudinal and transversal strains.

4. Results and discussion

4.1. Morphology

Figs 1 and 2 present the scanning electron micrographs of syntactic foams filled with 40% by volume of, respectively, K25 and 110P8CP00 microspheres. The pictures do not exhibit any air bubbles whatever the microsphere nature is. Glass microspheres appear well dispersed in the matrix, which assesses the efficiency of the mixture process used. Few broken microspheres are visible but we cannot discuss SEM pictures in terms of crushed microsphere content since microspheres crushed during foam processing could not be distinguished from microspheres crushed during sample preparation (cryofracture).

We could check the size distribution of the microspheres as reported in Table II from technical data sheets. Note that we cannot observe in these pictures the epoxy-amine nodules expected in the matrix (average diameter of 1.5 microns [13]). Nevertheless, differential scanning calorimetry measurements allowed us to determine the glass transition temperatures associated with both phases, namely 205°C for PPE rich phase and 155°C for the fully cured thermoset rich phase, which were within the expected temperature ranges [13].

The amount of broken microspheres measured in weight % on syntactic foams including 40% in volume of various microspheres under study are reported in Table III.

Values measured appear quite sensitive to the microsphere nature. In comparison to syntactic foams including S38 and S60 microspheres, the higher level of broken microspheres obtained in presence of K25 is not surprising considering the typical isostatic crush strength of the neat microspheres given in Table II. On the contrary, such level of crushed microsphere was not expected in the case of 110P8CP00 ones, and could influence final properties. However, we should also take into account the initial amount of crushed microspheres that may lead to an overestimation of the content of crushed microsphere due to the process. In conclusion, the innovative process of syntactic foams developed can lead to satisfactorily materials when using adapted microspheres.

4.2. Elasticity at room temperature

Fig. 3 presents the plots of the Young's modulus at 21°C as a function of the microsphere volume fraction for the

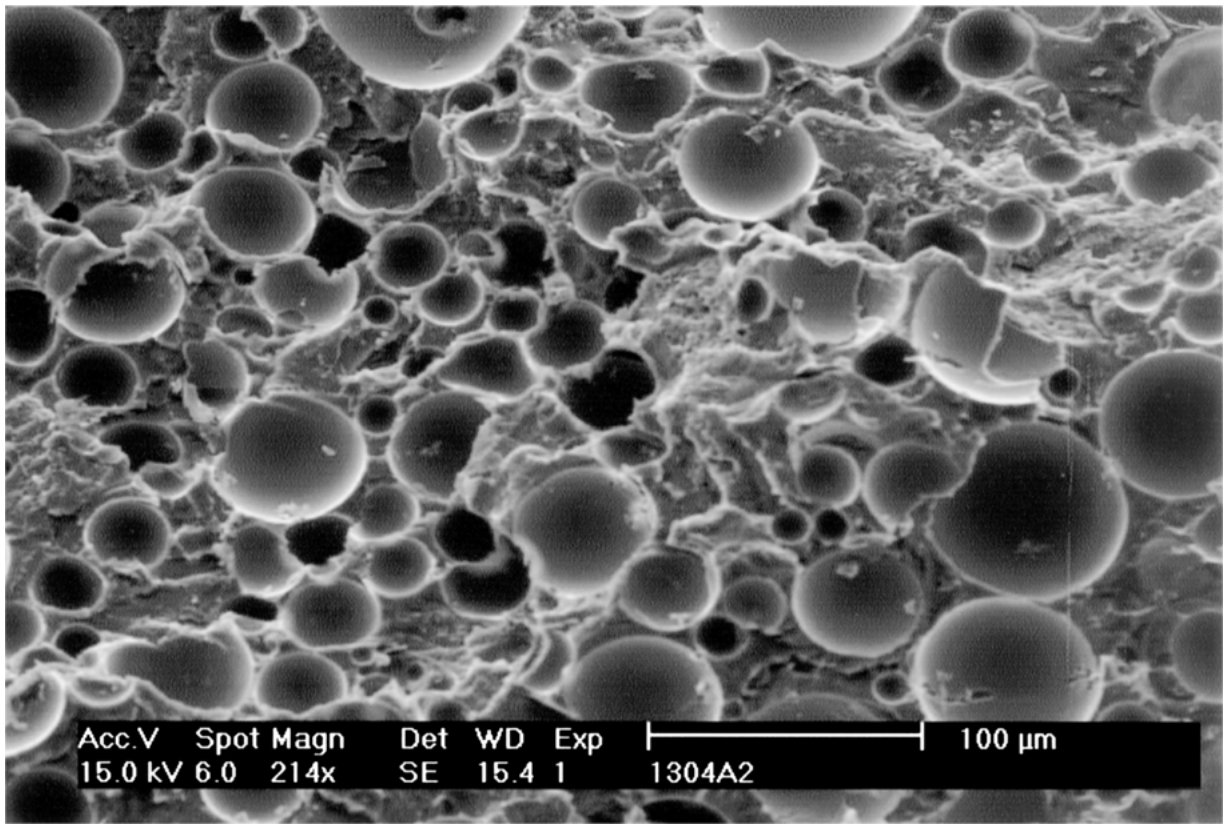

Figure 1 Scanning electron micrograph of a syntactic foam filled with 40% by volume of microspheres K25 (3M).

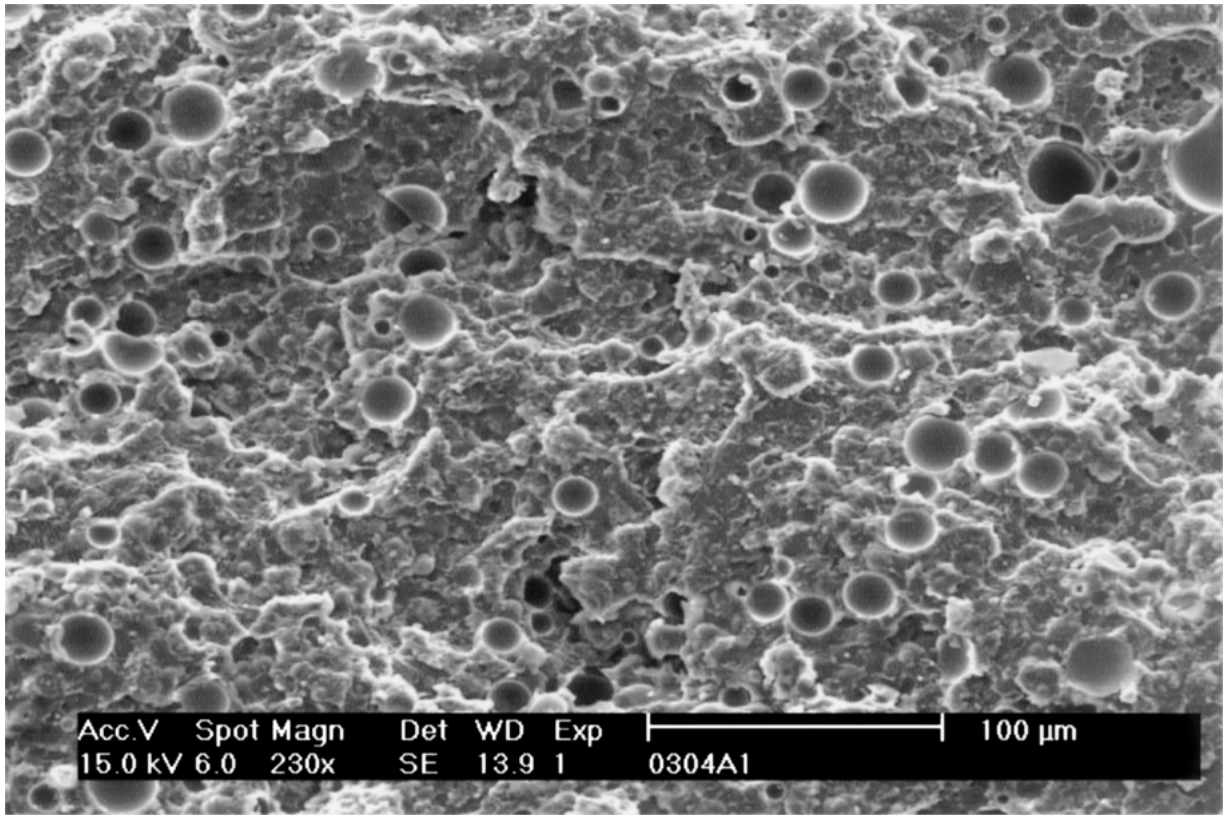

Figure 2 Scanning electron micrograph of a syntactic foam filled with 40% by volume of microspheres 110P8CP00 (Potters).

different syntactic foams under study. At a fixed volume fraction of microspheres, the composite elastic modulus clearly depends on the nature of the incorporated microspheres.

Similar observations reported in the literature were discussed in terms of the ratio between wall thickness and radius of the microsphere [14–18]. This geometrical parameter can easily be calculated from the true

TABLE III Content of broken microspheres in syntactic foams containing 40% by volume of microspheres

Syntactic foams	Content of broken microspheres (weight%)
PPE40/K25 40% vol.	13
PPE40/S38 40% vol.	6
PPE40/S60 40% vol.	6
PPE40/110P8CP00 40% vol.	10

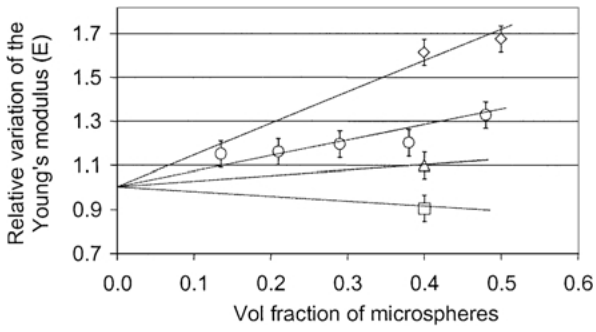

Figure 3 Evolution of the relative Young's modulus measured by uniaxial compression at 21°C as a function of microsphere volume fraction. ((◇) 110P8CP00, (◯) S60, (△) S38, and (□) K25).

density of a microsphere using Equation 1:

$$e/r = 1 - [1 - (\rho_{\text{true}}/\rho_{\text{G}})]^{1/3} \tag{1}$$

with e = wall thickness of the microspheres, r = average radius of the microspheres, ρ_{true} = true density of the microspheres, and ρ_{G} = density of the glass (2540 kg/m^3).

Wall thickness to radius ratios calculated for microspheres under study are given in Table IV.

In agreement with the literature, one can see from Fig. 3 that the elastic modulus decreases when microspheres exhibit a low wall thickness to radius ratio, while the modulus increases with microspheres exhibiting a higher wall thickness to radius ratio. The threshold where the elastic modulus of the composite material remains constant whatever the volume fraction of microspheres is expected for microspheres exhibiting a wall thickness to radius ratio between 0.034 and 0.053.

This observation is in agreement with the critical value of 0.035 calculated by Avena with a homogenisation approach [19]. Increasing the wall thickness to radius ratio means that the proportion of glass in the matrix is increasing and the proportion of voids is decreasing. A consequence is the existence of two limiting

TABLE IV Additional microsphere characteristics

Microsphere references	Wall thickness/ radius[a] e/r	Internal radius/ external radius $(r-e)/e$	Shear modulus of microsphere G_{H}^{b} (GPa)
K25	0.034	0.97	1.47
S38	0.053	0.95	2.30
S60	0.086	0.91	3.81
110P8CP00	0.172	0.83	7.87

[a]Calculated from Equation 1.
[b]Calculated from Equation 2.

situations: a wall thickness to radius ratio equal to 1 in the case of a composite material filled with glass beads and a wall thickness to radius ratio equal to 0 in the case of a cellular foam obtained with a blowing agent. In the first case, microspheres allow a reinforcing effect like most of the fillers do in polymers, whereas microspheres act as pores in the matrix in the second case. It is interesting to note that Huang *et al.* [15] have observed that the internal to external radius ratio is constant whatever the distribution of the microsphere is. Therefore, the wall thickness to radius ratio is a really pertinent parameter because it does not depend on the particle size distribution which is large. Modeling using finite elements have confirmed this analysis, though interfacial adhesion between microspheres and matrix has not been taken into account [15, 20].

One of the difficulties in modeling the elastic behavior of a syntactic foam is to estimate the Young's modulus of a hollow sphere. Nielsen [21] proposed to relate the apparent modulus of a hollow sphere to the power three of the ratio between outer and inner radii as shown in Equation 2.

$$\frac{G_{\text{H}}}{G_{\text{s}}} = \frac{1-(a/r)^3}{1+(a/r)^3} \tag{2}$$

with G_{H} = apparent shear modulus of a hollow glass sphere, G_{s} = shear modulus of a solid glass sphere (28.5 GPa), r = outer radius, and a = inner radius ($a = r - e$).

Shear moduli calculated from Equation 2 for microspheres under study are reported in Table IV. Knowing the microsphere modulus, it was then possible to test different equations proposed to fit the experimental elastic behavior for a two-phase system. In the three following models, PPE40 was considered as an homogeneous material of equivalent shear modulus equal to $G_{\text{m}} = 0.98$ GPa at room temperature.

The first equation (Equation 3) used to fit our experimental results is due to Kerner [22]:

$$\frac{G_{\text{c}}}{G_{\text{m}}} = \frac{1+AB\phi_{\text{f}}}{1-B\phi_{\text{f}}} \tag{3}$$

with

$$A = (7-5\nu_{\text{m}})/(8-10\nu_{\text{m}})$$
$$B = \frac{(G_{\text{H}}/G_{\text{m}})-1}{(G_{\text{H}}/G_{\text{m}})+A}$$

G_{c} = composite shear modulus, G_{m} = matrix equivalent shear modulus, ϕ_{f} = volume fraction of spheres, and ν_{m} = Poisson's ratio of the polymer matrix.

Kerner's model has been modified by Nielsen [21, 23]:

$$\frac{G_{\text{c}}}{G_{\text{m}}} = \frac{1+AB\phi_{\text{f}}}{1-B\psi\phi_{\text{f}}} \tag{4}$$

with

$$\Psi = 1 + \left[\left(1-\phi_{\text{f}}^{\max}\right)/\left(\phi_{\text{f}}^{\max}\right)^2\right]\phi_{\text{f}}$$

ϕ_f^{max} = maximum packing fraction of the filler phase (for uniform spheres: 0.64). The last model considered in this work was the one proposed by Sato-Furukawa [24] which includes an adjustable parameter (ξ) reflecting the adhesion between filler and matrix:

$$\frac{E_c}{E_m} = \left\{1 + \left[\frac{y^2}{2(1-y)}\right]\right\}(1 - \psi\xi) - \left[\frac{y^2\psi\xi}{(1-y)y^3}\right] \quad (5)$$

with

$$\phi_f = y^3, \quad \psi = \frac{(y^3/3)(1 + y - y^2)}{(1 - y + y^2)}$$

ξ = the adhesion parameter ($\xi = 0$ stands for a perfect adhesion and $\xi = 1$ means no adhesion).

In order to compare experimental Young's moduli to their modeled counterparts, elastic moduli were calculated from the shear moduli by means of the well-known equation:

$$E = 2G(1 + \nu) \quad (6)$$

with ν = the Poisson's coefficient.

The Poisson's coefficient measured for syntactic foams filled with different volume fractions of microspheres S60 was found to be roughly constant and equal to 0.35, and this value was used in the calculation.

Plots of experimental and modeled Young's modulus as a function of microsphere volume content are shown in Fig. 4 for PPE40/S60 syntactic foams.

According to the trends of predicted moduli versus microsphere content, both Kerner and Lewis-Nielsen models overestimate the experimental results. Palumbo *et al.* [14] found that the Sato-Furukawa model was the best for modeling their results. However, it seems difficult to discuss the Sato-Furukawa model because the adjustable parameter makes it easy to find a curve that fits the experimental data perfectly. As we said, all those models are dedicated to biphasic systems. But in our case, we actually have composites composed of a TP matrix, a dispersed phase (TS) and fillers (hollow spheres). Moreover, the amount of crushed microspheres due to the processing of the syntactic foams was neglected. Those approximations could explain the discrepancy between the measurements and the model predictions.

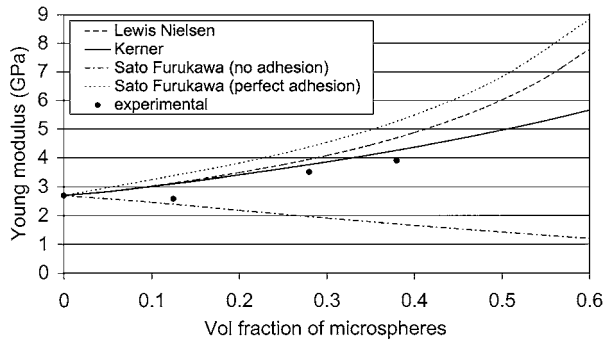

Figure 4 Comparison between experimental measurements and predictions for the Young's modulus E as a function of the volume fraction of filler, for a PPE40 matrix including S60 microspheres.

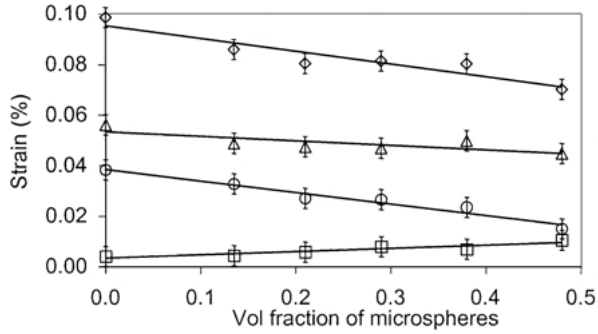

Figure 5 Evolution of the plastic (□), anelastic (◯), and elastic (Δ) parts of the strain (◇) as a function of the volume fraction of microspheres for syntactic foams based on PPE40/S60 (room temperature).

4.3. Elasticity, plasticity and anelasticity at the yield point (21°C)

Strain recoveries from the yield point at room temperature were compared for syntactic foams based on PPE40/S60 microspheres in order to distinguish the elastic strain, ε_{el}, which recovers instantaneously, the anelastic strain, ε_{an}, which recovers over a short period of time, and the plastic strain, ε_{pl}, which is permanent below T_g on the experimental time scale. Fig. 5 illustrates the results reported as a function of the volume fraction of microspheres.

We can see first that the plastic part of the yield strain remains below 1% whatever the composition is, which means that strain is almost completely recoverable before the yield point. The microspheres do not change strongly the behaviour of the polymeric material. Indeed, works on linear and semi-crystalline polymers [25] and for TP/TS blends [13] show that the anelastic deformation onsets from the very beginning of the compressive test and the stress peak develops when ε_{an} increases greatly, whereas the plastic deformation is just setting in. Secondly, we can observe that the anelastic part decreases with the increasing fraction of microspheres. For 50% in volume of microspheres, all the recoverable deformation is done almost instantaneously. This can be related to the fact that the proportion of the matrix is decreasing, the latter being responsible for the anelasticity because of its polymeric nature. This study of the different parts of the strain shows that it is extremely important to qualify the yield stress precisely to be sure that there is no remanent deformation.

4.4. Yielding behaviour

4.4.1. At room temperature

Fig. 6 presents plots of the yield stress at room temperature as a function of volume fraction of microspheres for the different syntactic foams under study.

In the case of syntactic foams filled with S60, the incorporation of microspheres has almost no influence on the yield stress whatever the compositions are. The yield stress just increases by 5 MPa with 50% vol of microspheres. However, at a fixed volume fraction of

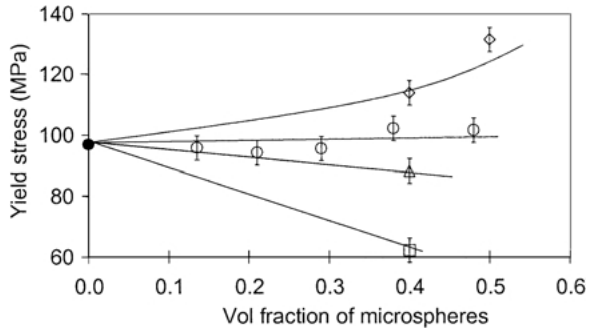

Figure 6 Influence of the volume fraction and the type of microsphere on the yield stress obtained by a uniaxial compression test at room temperature ($1.10^{-3}\Delta^{-1}$). ((◇) 110P8CP00, (◯) S60, (△) S38, (□) K25, (●) matrix).

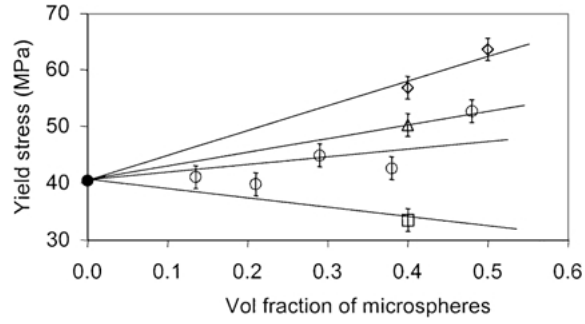

Figure 7 Influence of the volume fraction and the type of microsphere on the yield stress obtained by a uniaxial compression test at 150°C ($1.10^{-3}\Delta^{-1}$). ((◇) 110P8CP00, (◯) S60, (△) S38, (□) K25, (●) matrix).

microspheres, the type of microsphere has a strong influence on the ability of plastic deformation. As was stated about the elastic behaviour, the influence of the wall thickness to radius ratio plays a fundamental role.

4.4.2. At 150°C

Similar experiments were performed at 150°C in order to analyse the behaviour of syntactic foams in view of high temperature applications. Results are presented in Fig. 7.

As expected, the temperature increase induces a substantial drop in the yield stress values measured at 150°C whatever the composition is. Indeed, the T_g onset of the epoxy-amine phase is 155°C which is very close to the experimental temperature. However, the yield stress values remain above 30 MPa, corresponding to the hydrostatic pressure existing at 3,000 m depth. Thus, the syntactic foams under study could be used for their outstanding thermal performance down to what is called 'ultra deep water'.

These experiments have demonstrated that it is possible to design syntactic foams with specific microsphere and volume fraction to avoid the yielding of the syntactic foam in ultra deep water.

5. Conclusions

This study aims at validating an innovative process to provide syntactic foams with high temperature resistance for pipeline insulation up to 150°C. First, the reactive extrusion process was selected to process high T_g thermoplastics. Second, hollow glass microspheres were mixed with the thermoplastic based reactive blend at 175°C and led after cure to syntactic foams based on TP/TS matrix. Additional work has enabled the mixing process to be successfully upscaled by using a twin-screw extruder instead of a mixer. In both cases, attention was paid to the breakage level of microspheres during processing that could lead to a reduction in insulation performance. Besides, we want to stress that this new process uses classical processing means (e.g., a twin-screw extruder) and includes no Volatile Organic Compound, in agreement with environmental restrictions.

The results on the evaluation of mechanical properties reported here show that syntactic foams based on TP/TS matrix exhibit good performance at 150°C as expected from the matrix selection. In addition, the wall thickness to radius ratio is confirmed to be the key parameter that governs the mechanical properties of syntactic foams. These foams are expected to be used as thermal insulators for pipes. Unfortunatly it seems clear that (following the rule of mixture), the introduction of microsphere with high glass content (high *e*/*r* ratio) which is the best for high compressive mechanical properties is the worst for the thermal conductivity, and thus a balance has to be considered for technical applications. Further work is in progress to evaluate insulation and ageing properties (by the use of coupling agents) and to optimise the innovative syntactic foams developed.

Acknowledgements

The authors would like to thank the Institut Français du Pétrole for Financial support. The contributions of F. Fenouillot-Rimlinger, H. Perier Camby and J. Grenier (reactive extrusion) are gratefully acknowledged. The authors acknowledge D. Willepentoux of 3M for supplying microspheres.

References

1. F. A. SHUTOV, in "Handbook of Polymeric Foams and Foam Technology," edited by D. Klemper and K. C. Frisch (Hanser Publishers, Munich, Vienna, New York, Barcelona, 1991) p. 355.
2. A. LELU, G. FONTBLANC, J. M. BESSON, C. FILLIATRE and R. DAVIAUD, *Makromol. Chem, Makromol. Symp*. **9** (1987) 39.
3. E. DE ARAGÃO, PhD Thesis, University Bordeaux 1, 1986.
4. A. BONNET, J. P. PASCAULT, H. SAUTEREAU, M. TAHA and Y. CAMBERLIN, *Macromolecules* **32** (1999) 8517.
5. A. BONNET, J. P. PASCAULT, H. SAUTEREAU and Y. CAMBERLIN, *ibid.* **32** (1999) 8524.
6. R. VENDERBOSCH, PhD Thesis, University of Technology, Eindhoven, The Netherlands, 1995.
7. K. ASHIDA, in "Handbook of Plastics Foams," edited by Arthur H. Landrock (Noyes Publications, 1995) p. 147.
8. Shell Oil Compagny, Great Britain, Patent no. 5,158,727,1992-10-27.
9. Shell Research Limited, Great Britain, Patent no. 5,597,522,1997-01-28.
10. E. GIRARD-REYDET, H. SAUTEREAU, J. P. PASCAULT, P KEATES, P. NAVARD, G. THOLLET and G. VIGIER, *Polymer* **39** (1998) 2269.

11. J. P. PASCAULT and R. J. J. WILLIAMS in "Polymer Blends," edited by D. R. Paul and C. B. Bucknall (Interscience, New York, 2000) Vol. 1, p. 379.
12. S. PONCET, G. BOITEUX, J. P. PASCAULT, H. SAUTEREAU, G. SEYTRE, J. ROGOZINSKY and D. KRANBUEHL, *Polymer* **40** (1999) 6811.
13. A. BONNET, B. LESTRIEZ, J. P. PASCAULT and H. SAUTEREAU, *J. Polym. Sci.: Part B Polym. Phys*. **39** (2001) 363.
14. M. PALUMBO, G. DONZELLA, E. TEMPESTI and P. FERRUTI, *J. Appl. Polym. Sci*. **60** (1996) 47.
15. J. S. HUANG and L. J. GIBSON, *J. Mech. Solids* **41** (1993) 55.
16. A. CORIGLIANO, E. RIZZI and E. PAPA, *Comp. Sci. Tech*. **60** (2000) 2169.
17. *Idem.*, *Int. J. Sol. Stru*. **37** (2000) 5773.
18. J. R. M. D'ALMEIDA, *Comp. Sci. Tech*. **59** (1999) 2087.
19. A. AVENA, PhD thesis, Ecole Nationale des Mines de Paris, 1987.
20. G. L'HOSTIS and F. DEVRIES, *Comp. Part* B **29B** (1998) 351.
21. L. E. NIELSEN, *J. Polym. Sci.: Polym. Phys. Ed*. **21** (1983) 1567.
22. E. H. KERNER, *Proc. Phys. Soc. (London)* **69B** (1956) 808.
23. L. E. NIELSEN, *J. Appl. Phys*. **41** (1970) 4626.
24. *Idem.*, *J. Appl. Polym. Sci*. **10** (1966) 97.
25. R. QUINSON, J. PEREZ, Y. GERMAIN and J. M. MURRACIOLE, *Polymer* **41** (1995) 743.

Received 17 May 2002
and accepted 13 March 2003